PHYSICAL REVIEW D **93,** 035014 (2016)

Higgs boson-μ-τ coupling at high and low energy colliders

Ying-nan Mao[1] and Shou-hua Zhu[1,2,3]

[1]*Institute of Theoretical Physics and State Key Laboratory of Nuclear Physics and Technology, Peking University, Beijing 100871, China*

[2]*Collaborative Innovation Center of Quantum Matter, Beijing 100871, China*

[3]*Center for High Energy Physics, Peking University, Beijing 100871, China*

(Received 8 September 2015; published 16 February 2016)

There is no tree-level flavor changing neutral current (FCNC) in the standard model (SM) which contains only one Higgs doublet. If more Higgs doublets are introduced for various reasons, the tree-level FCNC would be inevitable, except that extra symmetry was imposed. Therefore, FCNC processes are an excellent probe for physics beyond the SM (BSM). In this paper, we study the lepton flavor violated decay processes $h \to \mu\tau$ and $\tau \to \mu\gamma$ induced by the Higgs boson-μ-τ vertex. For $\tau \to \mu\gamma$, its branching ratio is also related to the $ht\bar{t}$, $h\tau^+\tau^-$, and hW^+W^- vertices. We categorize the BSM into two scenarios for the Higgs boson coupling strengths near or away from the SM. For the latter scenario, we take the spontaneously broken two Higgs doublet model (the Lee model) as an example. We consider the constraints by recent data from the LHC and B factories, and we find that the measurements give weak constraints. At LHC run II, $h \to \mu\tau$ will be confirmed or will have a stricter limit set on its branching ratio. Accordingly, $\mathrm{Br}(\tau \to \mu\gamma) \lesssim \mathcal{O}(10^{-10} - 10^{-8})$ for general chosen parameters. For the positive case, $\tau \to \mu\gamma$ can be discovered with $\mathcal{O}(10^{10})$ τ pair samples at the SuperB factory, the Super τ-charm factory, and the new Z factory. The future measurements for $\mathrm{Br}(h \to \mu\tau)$ and $\mathrm{Br}(\tau \to \mu\gamma)$ will be used to distinguish these two scenarios or set strict constraints on the correlations among different Higgs couplings.

DOI: 10.1103/PhysRevD.93.035014

I. INTRODUCTION

In the standard model (SM), we can diagonalize the gauge couplings and the Yukawa couplings simultaneously; i.e., there is no flavor changing neutral current (FCNC) at tree level. In the quark sector, flavor changing neutral currents occur at loop level with the help of the Cabibbo-Kobayashi-Maskawa quark mixing matrix [1]. However, in the lepton sector, it is extremely suppressed by the Glashow-Iliopoulos-Maiani mechanism [2] in the SM due to the smallness of the neutrino mass. For example, for the lepton flavor violation (LFV) process $\ell_i \to \ell_j\gamma$,

$$\frac{\Gamma(\ell_i \to \ell_j\gamma)}{\Gamma(\ell_i \to \ell_j\nu_i\bar{\nu}_j)} = \frac{3\alpha}{32\pi}\left|\sum_k V_{ik}^* V_{jk}\frac{m_{\nu_k}^2}{m_W^2}\right|^2 \tag{1}$$

in the SM [3], where V_{ij} represents the Pontecorvo-Maki-Nakagawa-Sakata lepton mixing matrix [4] elements. With the data from neutrino oscillation [5], it is estimated to be

$$\mathrm{Br}(\mu \to e\gamma) \sim \mathcal{O}(10^{-56}) \quad \text{and}$$
$$\mathrm{Br}(\tau \to e(\mu)\gamma) \sim \mathcal{O}(10^{-55}\text{–}10^{-54}) \tag{2}$$

in the SM. It is far from the recent experimental upper limit [6,7],[1]

$$\mathrm{Br}(\tau \to e\gamma) < \begin{cases} 1.2 \times 10^{-7} & (\text{Belle}) \\ 3.3 \times 10^{-8} & (BABAR) \end{cases}, \quad \mathrm{Br}(\tau \to \mu\gamma) < \begin{cases} 4.5 \times 10^{-8} & (\text{Belle}) \\ 4.4 \times 10^{-8} & (BABAR) \end{cases},$$
$$\text{and} \quad \mathrm{Br}(\mu \to e\gamma) < 5.7 \times 10^{-13} \quad (\text{MEG}), \qquad \text{all at } 90\% \text{ C.L.} \tag{3}$$

and the near future sensitivities with the improvement of an order [8–11]. Therefore, the discovery of the signals $\ell_i \to \ell_j\gamma$ at future colliders would clearly indicate a new physics (NP) beyond the SM (BSM). Generally speaking, the FCNC process will be one of the best probes of the BSM for future hadron and electron-positron colliders [12].

In July 2012, a new boson was discovered at the LHC [13,14], and its properties are like those of a SM Higgs boson [15]. The Higgs-mediated LFV process is attractive because of a 2.4σ hint found by the CMS Collaboration [16] in the search for the $h \to \mu\tau$ process.[2] Assuming that the Higgs production cross section and the total decay

[1]For either B factory with $L \approx 0.5\ \mathrm{ab}^{-1}$ luminosity at $\sqrt{s} = 10.6$ GeV [$\Upsilon(4S)$ threshold].

[2]Recently, the ATLAS Collaboration also published the searching result in the same process [17], with the result close to that in [16] by the CMS Collaboration.

width are the same as those in the SM, the best fit (B.F.) branching ratio and the 95% upper limit (U.L.) are, respectively [16],[3]

$$\begin{aligned} &\mathrm{Br}(h \to \mu\tau) = (0.84^{+0.39}_{-0.37})\% \quad \text{(B.F.)} \\ \text{and} \quad &\mathrm{Br}(h \to \mu\tau) < 1.51\% \text{(U.L.)}. \end{aligned} \tag{4}$$

If this signature were confirmed at future colliders, it would clearly indicate a NP in the Higgs sector. In the extensions of SM, there may be direct Higgs boson-μ-τ coupling to explain this hint, for example, in some types of two Higgs doublet models (2HDMs) [18], like type III 2HDM [19–22], 2HDMs with other flavor symmetries [23–25], the Lee model [26,27], and other models [28–30]. It may also be related to other phenomena, like the excess in $t\bar{t}h$ searches [31], $b \to s$ semileptonic decays [24], the anomalous magnetic moment $(g-2)$ for μ [32], LFV τ decays [21,25,32–34], and even the lepton flavored dark matter [35]. Writing the Higgs boson-μ-τ vertex as

$$\mathcal{L}_{h\mu\tau} = -\frac{h}{\sqrt{2}}(Y_{\mu\tau}\bar{\mu}_L\tau_R + Y_{\tau\mu}\bar{\tau}_L\mu_R + \mathrm{H.c.}) \tag{5}$$

and adopting the Cheng-Sher ansatz [36], the data gave [16]

$$\sqrt{|Y_{\mu\tau}|^2 + |Y_{\tau\mu}|^2} < 5 \times 10^{-3} \quad \text{or} \quad \sqrt{\frac{(|Y_{\mu\tau}|^2 + |Y_{\tau\mu}|^2)v^2}{2m_\mu m_\tau}} < 2. \tag{6}$$

In the future, at low energy e^+e^- colliders like the SuperB factory [9,10], the Super τ-charm factory [37,38], or the new Z factory [39], there would be signatures or stricter constraints for the $\tau \to \mu\gamma$ process, and at high energy colliders like the LHC run II at $\sqrt{s} =$ (13 to 14) TeV, there would be signatures or stricter constraints for the $h \to \mu\tau$ process. The results would be comparable and may put new constraints on the Higgs boson-μ-τ coupling or the correlations among the couplings between the Higgs boson and other particles.

This paper is organized as follows. In Sec. II we present the effective interactions and branching ratios for the $h \to \mu\tau$ and $\tau \to \mu\gamma$ processes; Secs. III and IV contain the constraints from recent data and at future colliders, respectively; and Sec. V includes our conclusions and a discussion.

II. EFFECTIVE HIGGS BOSON-μ-τ INTERACTION AND DECAY WIDTHS FOR $h \to \mu\tau$ AND $\tau \to \mu\gamma$ PROCESSES

Based on the 2HDM (type III), the Higgs effective couplings can be written as

$$\begin{aligned} \mathcal{L}_h = {} & c_V h\left(\frac{2m_W^2}{v}W^{+\mu}W^-_\mu + \frac{m_Z^2}{v}Z^\mu Z_\mu\right) \\ & - h\left(\frac{c_t m_t}{v}\bar{t}_L t_R + \frac{c_\tau m_\tau}{v}\bar{\tau}_L\tau_R + \mathrm{H.c.}\right) \\ & - \frac{h}{\sqrt{2}}(Y_{\mu\tau}\bar{\mu}_L\tau_R + Y_{\tau\mu}\bar{\tau}_L\mu_R + \mathrm{H.c.}), \end{aligned} \tag{7}$$

where c_i stands for the coupling strength ratio compared with that in the SM[4] and Y_{ij} stands for the LFV coupling just like that in Eq. (5). With a direct calculation [16], for the $h \to \mu\tau$ process, we have

$$\mathrm{Br}(h \to \mu\tau) = \frac{m_h}{16\pi\Gamma_h}(|Y_{\mu\tau}|^2 + |Y_{\tau\mu}|^2), \tag{8}$$

where Γ_h means the total decay width of Higgs boson, and in the SM we have $\Gamma_{h,\mathrm{SM}} = 4.1$ MeV [40] for $m_h = 125$ GeV.

The $\tau \to \mu\gamma$ decay process is loop induced. The dominant contribution usually comes from Barr-Zee-type[5] two-loop diagrams since there is an additional $(m_\tau/m_h)^2\log(m_h^2/m_\tau^2) \sim \mathcal{O}(10^{-3})$ suppression in the one-loop amplitude [42]; see the Feynman diagrams in Fig. 1. Following the formulas in [42],

$$\frac{\mathrm{Br}(\tau \to \mu\gamma)}{\mathrm{Br}(\tau \to \mu\nu\bar{\nu})} = \frac{48\pi^3\alpha}{G_F^2}(|\mathcal{A}_L|^2 + |\mathcal{A}_R|^2). \tag{9}$$

Here the left- (right-) handed amplitudes $\mathcal{A}_{L(R)}$ can be expressed as [20,32,42,43][6]

$$\begin{aligned} &\mathcal{A}_L(\mathcal{A}_R^*) \\ &= \mathcal{A}_{L,1\text{-loop}}(\mathcal{A}^*_{R,1\text{-loop}}) + \mathcal{A}_{L,2\text{-loop}}(\mathcal{A}^*_{R,2\text{-loop}}) \\ &= \frac{Y_{\mu\tau}(Y^*_{\tau\mu})}{16\sqrt{2}\pi^2}\left(\frac{m_\tau}{m_h^2 v}\left(c_\tau \ln\left(\frac{m_h^2}{m_\tau^2}\right) - \frac{4}{3}\mathrm{Re}(c_\tau) - \frac{5i}{3}\mathrm{Im}(c_\tau)\right)\right. \\ &\quad + \frac{c_V\alpha}{\pi m_\tau v}\left(\left(3 + \frac{m_h^2}{2m_W^2}\right)f\left(\frac{m_W^2}{m_h^2}\right)\right. \\ &\quad \left. + \left(\frac{23}{4} - \frac{m_h^2}{2m_W^2}\right)g\left(\frac{m_W^2}{m_h^2}\right) + \frac{3}{4}h\left(\frac{m_W^2}{m_h^2}\right)\right) \\ &\quad \left. - \frac{8\alpha}{3\pi m_\tau v}\left(\mathrm{Re}(c_t)f\left(\frac{m_t^2}{m_h^2}\right) + i\mathrm{Im}(c_t)g\left(\frac{m_t^2}{m_h^2}\right)\right)\right), \end{aligned} \tag{10}$$

[3]For the full LHC run I data with $L \approx 25$ fb^{-1} luminosity at $\sqrt{s} =$ (7–8) TeV.

[4]c_t and c_τ may be complex, while c_V must be real, and in the SM, $c_V = c_t = c_\tau = 1$.

[5]This type of two-loop diagrams was first proposed by Barr and Zee [41] during the calculation for the lepton electric dipole moment.

[6]The results in these papers are different. We checked the calculations and got a result consistent with that in [32], by Omura *et al.*

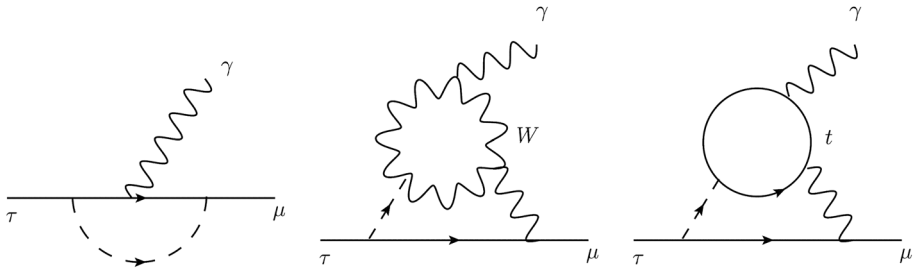

FIG. 1. Typical Feynman diagrams which contribute to the $\tau \to \mu\gamma$ decay. The left panel is a Higgs-mediated one-loop diagram, the middle and right panels are the W boson and top quark mediated Barr-Zee-type two-loop diagrams, respectively.

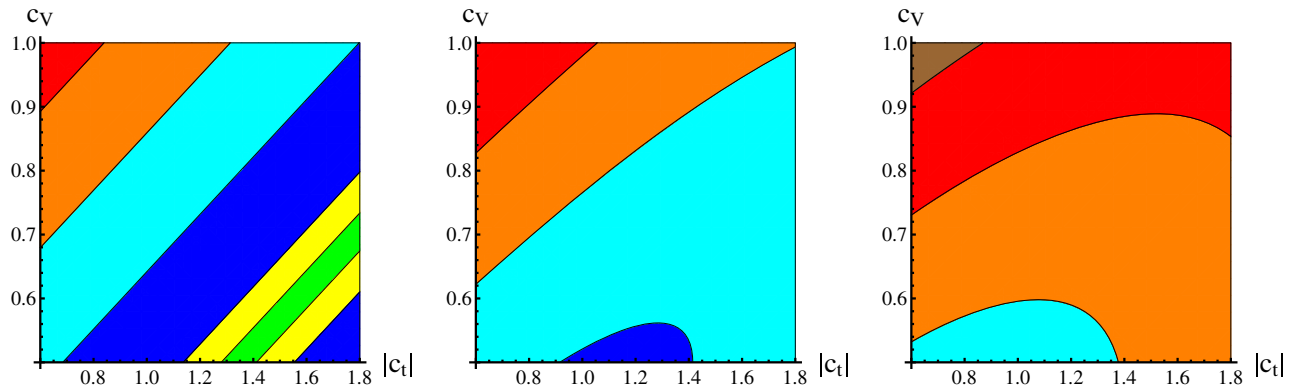

FIG. 2. Distribution for $R \equiv \mathrm{Br}(\tau \to \mu\gamma)/\mathrm{Br}(h \to \mu\tau)$ in the $c_V - |c_t|$ plane in the unit of $(\Gamma_{h,\mathrm{tot}}/\mathrm{MeV})$ fixing $c_\tau = 1$. We take $\alpha_t = (0, \pi/10, \pi/6)$ from left to right. The green regions are for $R < 10^{-10}$; the yellow regions are for $10^{-10} \le R < 10^{-9}$; the blue regions are for $10^{-9} \le R < 10^{-8}$; the cyan regions are for $10^{-8} \le R < 3 \times 10^{-8}$; the orange regions are for $3 \times 10^{-8} \le R < 6 \times 10^{-8}$; the red regions are for $6 \times 10^{-8} \le R < 10^{-7}$; and the brown regions are for $10^{-7} \le R < 1.5 \times 10^{-7}$.

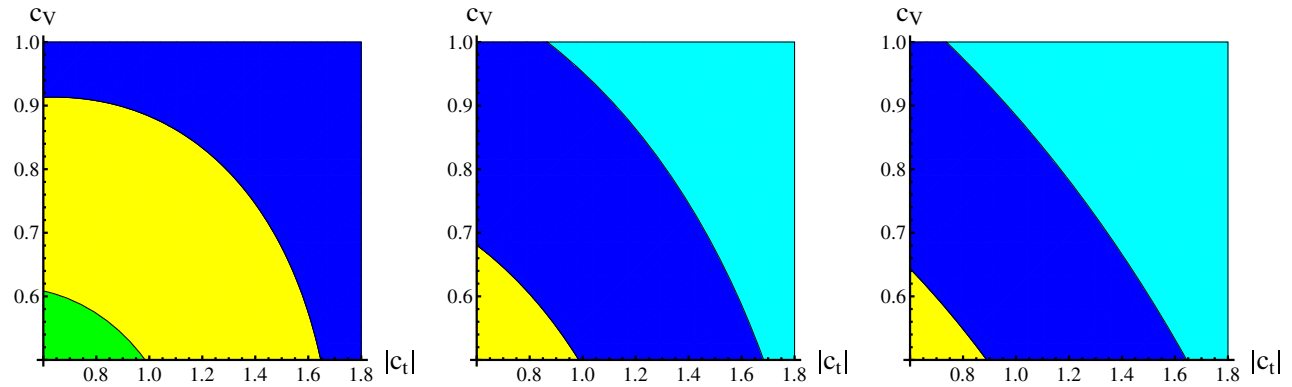

FIG. 3. Distribution for $R \equiv \mathrm{Br}(\tau \to \mu\gamma)/\mathrm{Br}(h \to \mu\tau)$ in the $c_V - |c_t|$ plane in the unit of $(\Gamma_{h,\mathrm{tot}})/\mathrm{MeV})$ fixing $c_\tau = 1$. We take $\alpha_t = (\pi/4, \pi/2, 2\pi/3)$ from left to right. The green regions are for $R < 10^{-7}$; the yellow regions are for $10^{-7} \le R < 2 \times 10^{-7}$; the blue regions are for $2 \times 10^{-7} \le R < 4 \times 10^{-7}$; and the cyan regions are for $4 \times 10^{-7} \le R < \times 10^{-6}$.

where all of the functions f, g, and h come from two-loop integrations as [43]

$$f(z) = \frac{z}{2}\int_0^1 dx \frac{1-2x(1-x)}{x(1-x)-z}\ln\left(\frac{x(1-x)}{z}\right), \quad (11)$$

$$g(z) = \frac{z}{2}\int_0^1 dx \frac{1}{x(1-x)-z}\ln\left(\frac{x(1-x)}{z}\right), \quad (12)$$

$$h(z) = -\frac{z}{2}\int_0^1 dx \frac{1}{x(1-x)-z} \times \left(1 - \frac{z}{x(1-x)-z}\ln\left(\frac{x(1-x)}{z}\right)\right). \quad (13)$$

The small contributions from the heavy neutral Higgs bosons, the charged Higgs boson, and the Z-mediated loop are all ignored. Defining

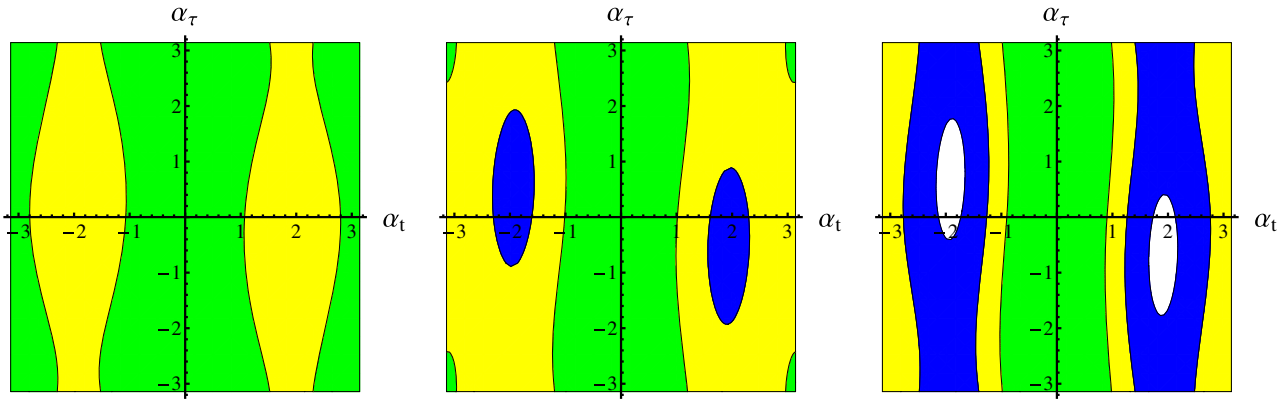

FIG. 4. $\mathrm{Br}(\tau \to \mu\gamma)$ distributions in the $\alpha_t - \alpha_\tau$ plane for $c_V = \Gamma_h/\Gamma_{h,\mathrm{SM}} = 1$, taking $|c_t| = 0.6, 1.2, 1.8$ from left to right. The green regions are for $\mathrm{Br}(\tau \to \mu\gamma) < 1.5 \times 10^{-8}$, the yellow regions are for $1.5 \times 10^{-8} \leq \mathrm{Br}(\tau \to \mu\gamma) < 3.0 \times 10^{-8}$, and the blue regions are for $3.0 \times 10^{-8} \leq \mathrm{Br}(\tau \to \mu\gamma) < 4.5 \times 10^{-8}$. White regions have already been excluded by recent data.

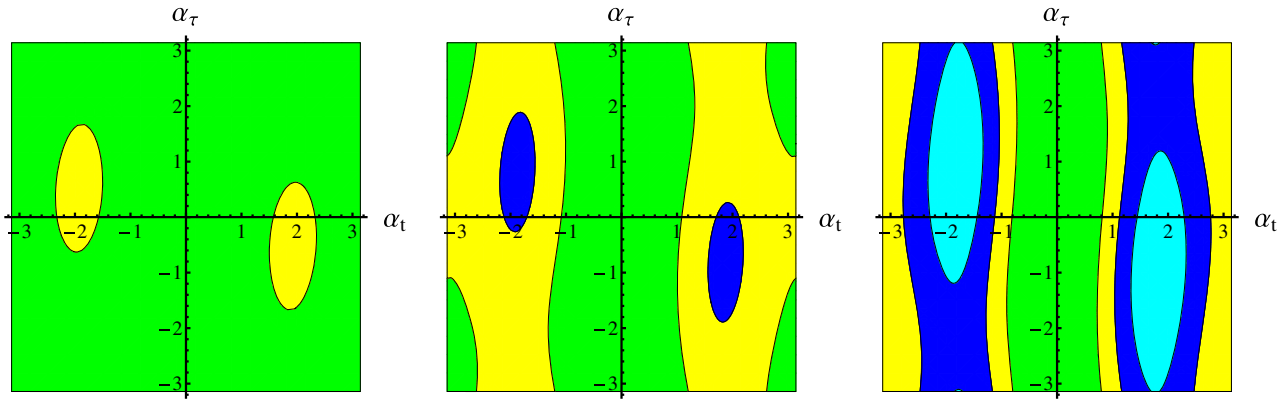

FIG. 5. $\mathrm{Br}(\tau \to \mu\gamma)$ distributions in the $\alpha_t - \alpha_\tau$ plane for $c_V = 0.5$, $\Gamma_h/\Gamma_{h,\mathrm{SM}} = 0.3$, taking $|c_t| = 0.6, 1.2, 1.8$ from left to right. The green regions are for $\mathrm{Br}(\tau \to \mu\gamma) < 2.5 \times 10^{-9}$, the yellow regions are for $2.5 \times 10^{-9} \leq \mathrm{Br}(\tau \to \mu\gamma) < 5 \times 10^{-9}$, the blue regions are for $5 \times 10^{-9} \leq \mathrm{Br}(\tau \to \mu\gamma) < 7.5 \times 10^{-9}$, and the cyan regions are for $7.5 \times 10^{-9} \leq \mathrm{Br}(\tau \to \mu\gamma) < 1 \times 10^{-8}$.

$$\mathcal{A} \equiv \frac{\mathcal{A}_L}{Y_{\mu\tau}} = \frac{\mathcal{A}_R}{Y_{\tau\mu}}, \tag{14}$$

Eq. (9) should be changed to

$$\frac{\mathrm{Br}(\tau \to \mu\gamma)}{\mathrm{Br}(\tau \to \mu\nu\bar{\nu})} = \frac{48\pi^3\alpha|\mathcal{A}|^2}{G_F^2}(|Y_{\mu\tau}|^2 + |Y_{\tau\mu}|^2). \tag{15}$$

Here, $\mathrm{Br}(\tau \to \mu\nu\bar{\nu}) = 17.4\%$ from PDG [5].

For both decay processes, the LFV parameter comes in the form $\sqrt{|Y_{\mu\tau}|^2 + |Y_{\tau\mu}|^2}$. Thus, we do not need to study the details about the chiral properties of the LFV coupling. Since $\mathrm{Br} \propto (|Y_{\mu\tau}|^2 + |Y_{\tau\mu}|^2)$, the ratio $\mathrm{Br}(\tau \to \mu\gamma)/\mathrm{Br}(h \to \mu\tau)$ does not depend on $Y_{\mu\tau(\tau\mu)}$. Therefore, in this paper we will focus on the correlations among the Higgs couplings.

III. CONSTRAINTS BY RECENT EXPERIMENTS

In general cases, $\alpha_t \equiv \arg(c_t)$ and $\alpha_\tau \equiv \arg(c_\tau)$ may be nonzero. The replacement

$$\mathrm{Br}(h \to \mu\tau) \to \frac{\sigma_h}{\sigma_{h,\mathrm{SM}}}\mathrm{Br}(h \to \mu\tau) = (\cos^2\alpha_t + 2.31\sin^2\alpha_t)\mathrm{Br}(h \to \mu\tau) \tag{16}$$

should also be taken into account in (4), where σ_h stands for the Higgs production cross section[7] and $\sigma_{h,\mathrm{SM}}$ represents it in SM. To consider the numerical constraints on the couplings in (7), we should take some benchmark points. Our fitting results [26] preferred $|c_\tau| \sim 1$ over almost all other chosen parameters, so in this paper we take $|c_\tau| = 1$. The regions $c_V \lesssim 0.4$, $|c_t| \lesssim 0.5$, and $|c_t| \gtrsim 2$ are excluded for most cases by our fitting results, so we never consider those regions in this paper.

According to (10), $R \equiv \mathrm{Br}(\tau \to \mu\gamma)/\mathrm{Br}(h \to \mu\tau)$ is sensitive to the interplay between c_V and c_t. The cancellation between W loop and t loop induced amplitudes would make R very small in some regions, especially for $\alpha_t \sim 0$. In Figs. 2 and 3, we show some $R \equiv \mathrm{Br}(\tau \to \mu\gamma)/\mathrm{Br}(h \to \mu\tau)$

[7]The gluon fusion process is dominant in this case.

TABLE I. Choices for typical Br($\tau \to \mu\gamma$)'s in different cases.

	Result at SuperB	Result at Super τ-charm	Typical choice on Br($\tau \to \mu\gamma$)
Case I	positive	positive	$\sim 10^{-8}$
Case II	negative	positive	$\sim 10^{-9}$
Case III	negative	negative	$\lesssim 2 \times 10^{-10}$

distribution in the $c_V - |c_t|$ plane in units of $(\Gamma_{h,\mathrm{tot}}/\mathrm{MeV})$ for some different α_t's. From the figures, we can also see the cancellation behavior clearly when α_t is small. For larger α_t's, the imaginary parts of the amplitudes would give more important contributions, and the imaginary parts of the one-loop contribution would also become more important, as the latter figures show.

Here and in the following sections, we categorize BSM into two scenarios. In scenario I, we choose most Higgs couplings close to those in the SM, especially $c_V \sim 1$ and $\Gamma_h/\Gamma_{h,\mathrm{SM}}$. Since the experimental data [15] are consistent with the SM predictions, this scenario is popular. In addition, the data still allow for Higgs couplings other than those in the SM, and these scenarios are attractive because they are strongly related to BSM physics. In scenario II, we choose the Lee model [26,27] as such a benchmark model. Our previous work [26] showed that there is no SM limit for the lightest scalar in the Lee model. We take the 125 GeV Higgs boson as the lightest one, so some of its couplings must be apart from those in the SM; it is especially important that c_V be small. In that paper, we considered full constraints by data and showed it is still alive. The fitting results for Higgs signal strengths allowed $c_V \sim 0.5$ and, at the same time, $|c_b|$ and Γ_h must be smaller than those in the SM. The results are not sensitive to the charged Higgs loop contribution. Typically, $\Gamma_h/\Gamma_{h,\mathrm{SM}} \sim \mathcal{O}(0.1)$ for different $|c_b|$ choices. In both scenarios, $|c_t| \sim |c_\tau| \sim 1$ is preferred.

In scenario I, we take $|c_t| = 0.6$, 1.2, 1.8 and plot the predicted branching ratios for $\tau \to \mu\gamma$ in Fig. 4, with $c_V = \Gamma_h/\Gamma_{h,\mathrm{SM}} = 1$, assuming $\mathrm{Br}(h \to \mu\tau) = 1.51\%$ as the CMS upper limit. White regions have already been excluded by recent data. For $|c_t| < 1.7$, all of the choices for (α_t, α_τ) are still allowed by recent data using this set of benchmark points. Thus, the recent $\tau \to \mu\gamma$ measurements cannot give further constraints. While in scenario II the predicted branching ratios for $\tau \to \mu\gamma$ are highly suppressed to be of $\mathcal{O}(10^{-9})$, the Lee model is not constrained by recent data. We take $|c_t| = 0.6$, 1.2, 1.8 again and plot the

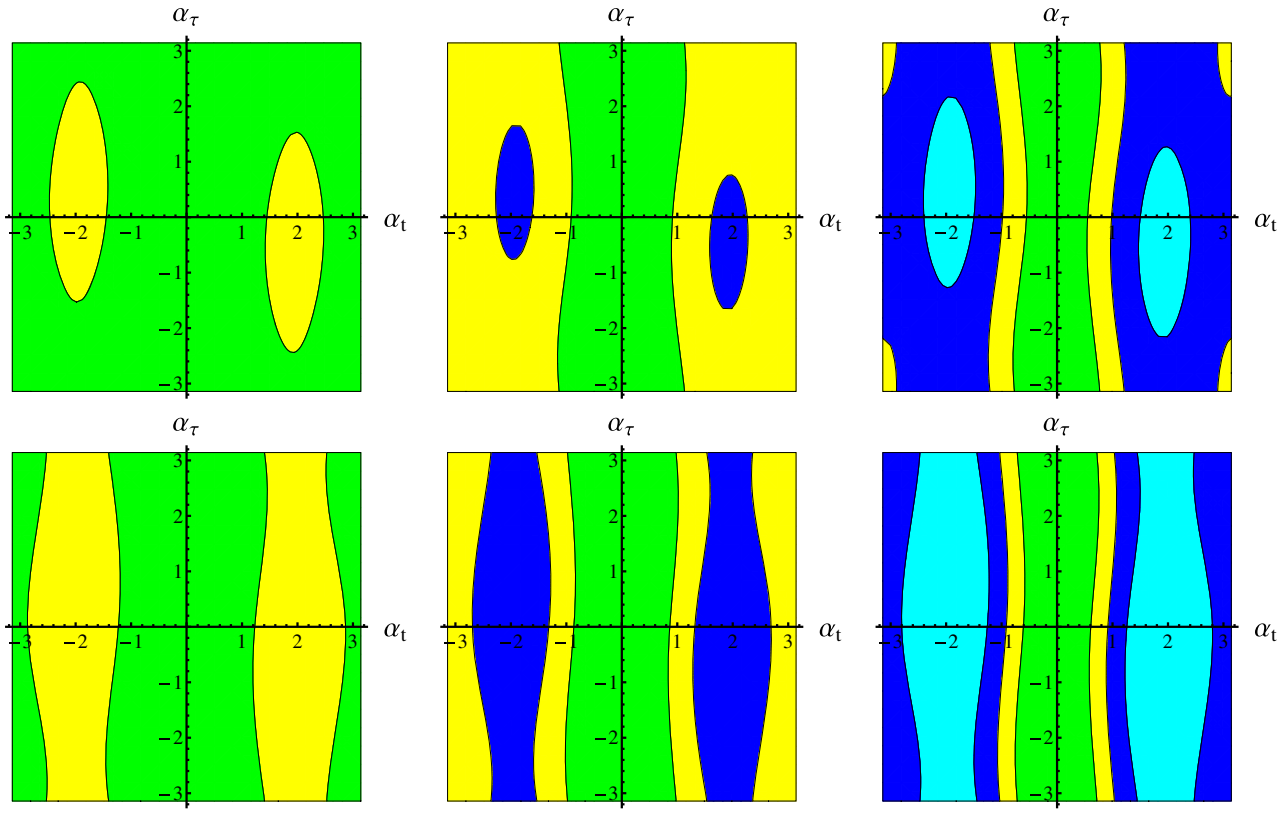

FIG. 6. Br($\tau \to \mu\gamma$) distributions in the $\alpha_t - \alpha_\tau$ plane for $c_V = \Gamma_h/\Gamma_{h,\mathrm{SM}} = 1$, taking $|c_t| = 1$ in the first line and $|c_t| = 1.5$ in the second line, and $(\sigma_h/\sigma_{h,\mathrm{SM}})\mathrm{Br}(h \to \mu\tau) = (1.5, 3, 6) \times 10^{-3}$ from left to right. The green regions are for $\mathrm{Br}(\tau \to \mu\gamma) < 2.4 \times 10^{-9}$, the yellow regions are for $2.4 \times 10^{-9} \le \mathrm{Br}(\tau \to \mu\gamma) < 5.4 \times 10^{-9}$, the blue regions are for $5.4 \times 10^{-9} \le \mathrm{Br}(\tau \to \mu\gamma) < 1 \times 10^{-8}$, and the cyan regions are for $\mathrm{Br}(\tau \to \mu\gamma) \ge 1 \times 10^{-8}$.

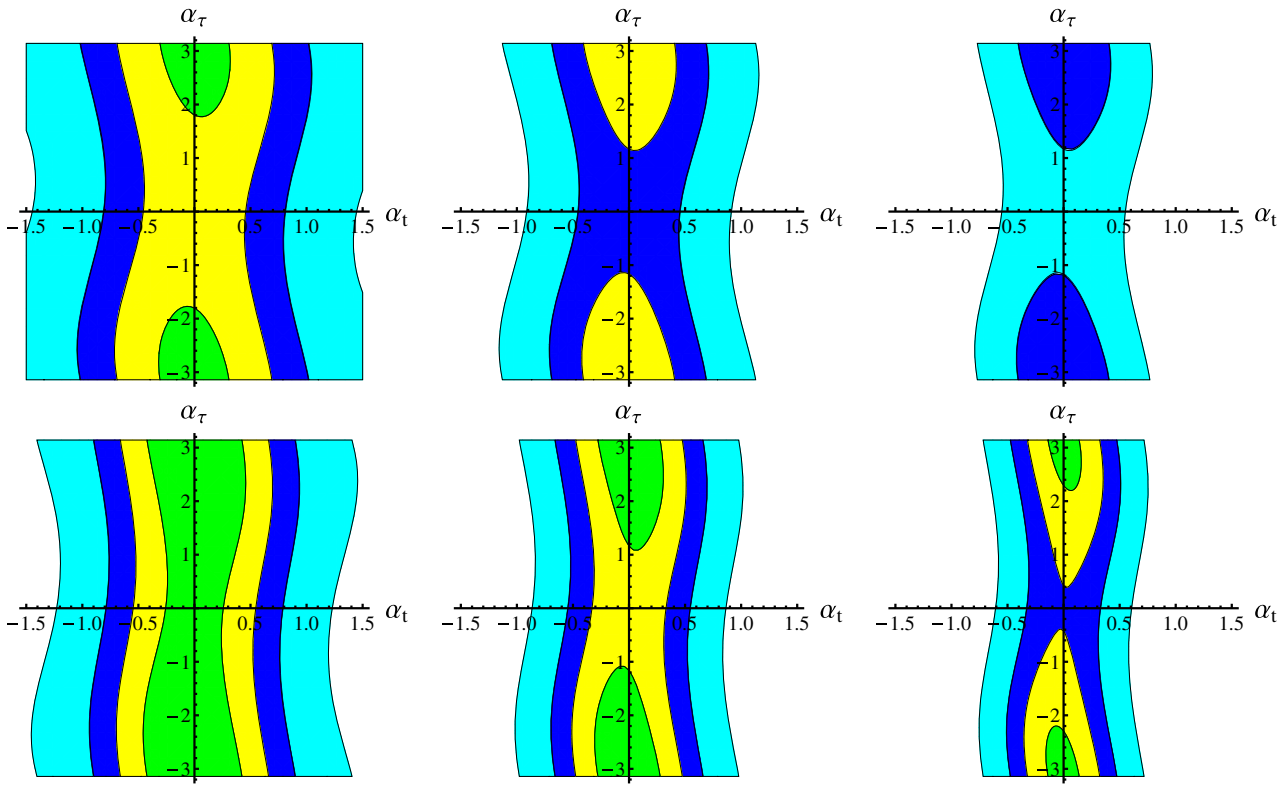

FIG. 7. $\mathrm{Br}(\tau \to \mu\gamma)$ distributions in the $\alpha_t - \alpha_\tau$ plane for $c_V = \Gamma_h/\Gamma_{h,\mathrm{SM}} = 1$, taking $|c_t| = 1$ in the first line and $|c_t| = 1.5$ in the second line, and $(\sigma_h/\sigma_{h,\mathrm{SM}})\mathrm{Br}(h \to \mu\tau) = (1.5, 3, 6) \times 10^{-3}$ (from left to right). The green regions are for $\mathrm{Br}(\tau \to \mu\gamma) < 2 \times 10^{-10}$, the yellow regions are for $2 \times 10^{-10} \leq \mathrm{Br}(\tau \to \mu\gamma) < 5 \times 10^{-10}$, the blue regions are for $5 \times 10^{-10} \leq \mathrm{Br}(\tau \to \mu\gamma) < 10^{-9}$, and the cyan regions are for $10^{-9} \leq \mathrm{Br}(\tau \to \mu\gamma) < 2.4 \times 10^{-9}$.

predicted $\mathrm{Br}(\tau \to \mu\gamma)$ in the Lee model in Fig. 5, with $c_V = 0.5$ and $\Gamma_h/\Gamma_{h,\mathrm{SM}} = 0.3$, assuming $\mathrm{Br}(h \to \mu\tau) = 1.51\%$ as the CMS upper limit.

IV. CONSTRAINTS AT FUTURE COLLIDERS

Kopp and Nardecchia [44] studied the phenomenology of $h \to \mu\tau$ at the future LHC ($\sqrt{s} = 13$ TeV). With 300 fb^{-1} luminosity, their results showed that for $\sigma_h = \sigma_{h,\mathrm{SM}}$, if no signal is observed, the expected upper limit at 95% C.L. should be set as $\mathrm{Br}(h \to \mu\tau) < 7.7 \times 10^{-4}$ [44], which means that

$$\sqrt{|Y_{\mu\tau}|^2 + |Y_{\tau\mu}|^2} < 1.1 \times 10^{-3}$$
$$\text{or} \quad \sqrt{\frac{(|Y_{\mu\tau}|^2 + |Y_{\tau\mu}|^2)v^2}{2m_\mu m_\tau}} < 0.45. \tag{17}$$

On the other hand, a signal would be observed at over 3σ if $\mathrm{Br}(h \to \mu\tau) > 1.3 \times 10^{-3}$, which means that

$$\sqrt{|Y_{\mu\tau}|^2 + |Y_{\tau\mu}|^2} > 1.5 \times 10^{-3}$$
$$\text{or} \quad \sqrt{\frac{(|Y_{\mu\tau}|^2 + |Y_{\tau\mu}|^2)v^2}{2m_\mu m_\tau}} > 0.59. \tag{18}$$

The SuperB factory is an e^+e^- collider at the $\Upsilon(4S)$ threshold with the luminosity 75 ab^{-1}. For the LFV decay $\tau \to \mu\gamma$, if no signal was observed at the SuperB factory, the expected upper limit at 90% C.L. should be set as [10]

$$\mathrm{Br}(\tau \to \mu\gamma) < 2.4 \times 10^{-9}. \tag{19}$$

On the other hand, a signal would be observed at over 3σ if

$$\mathrm{Br}(\tau \to \mu\gamma) > 5.4 \times 10^{-9}. \tag{20}$$

At the Super τ-charm factory, which is an e^+e^- collider at $\sqrt{s} = (2\text{–}7)$ GeV with the luminosity 10 ab^{-1}, there would be about 2.5×10^{10} pairs of $\tau^+\tau^-$'s [38]. The sensitivity for the LFV decay $\tau \to \mu\gamma$ would be of $\mathcal{O}(10^{-10})$ [38] because of the suppression in the background compared with that at the SuperB factory.[8] The same sensitivity $[\sim\mathcal{O}(10^{-10})]$ would also be achieved at the new Z factory [39] with the $\mathcal{O}(10^{12})$ Z bosons.

[8]The dominant backgrounds come from $\tau^+\tau^-\gamma$ events with a hard enough photon at the SuperB factory, while at the Super τ-charm factory, $\sqrt{s}$ is not far above the $\tau^+\tau^-$ threshold where almost all of the photons from $\tau^+\tau^-\gamma$ are soft.

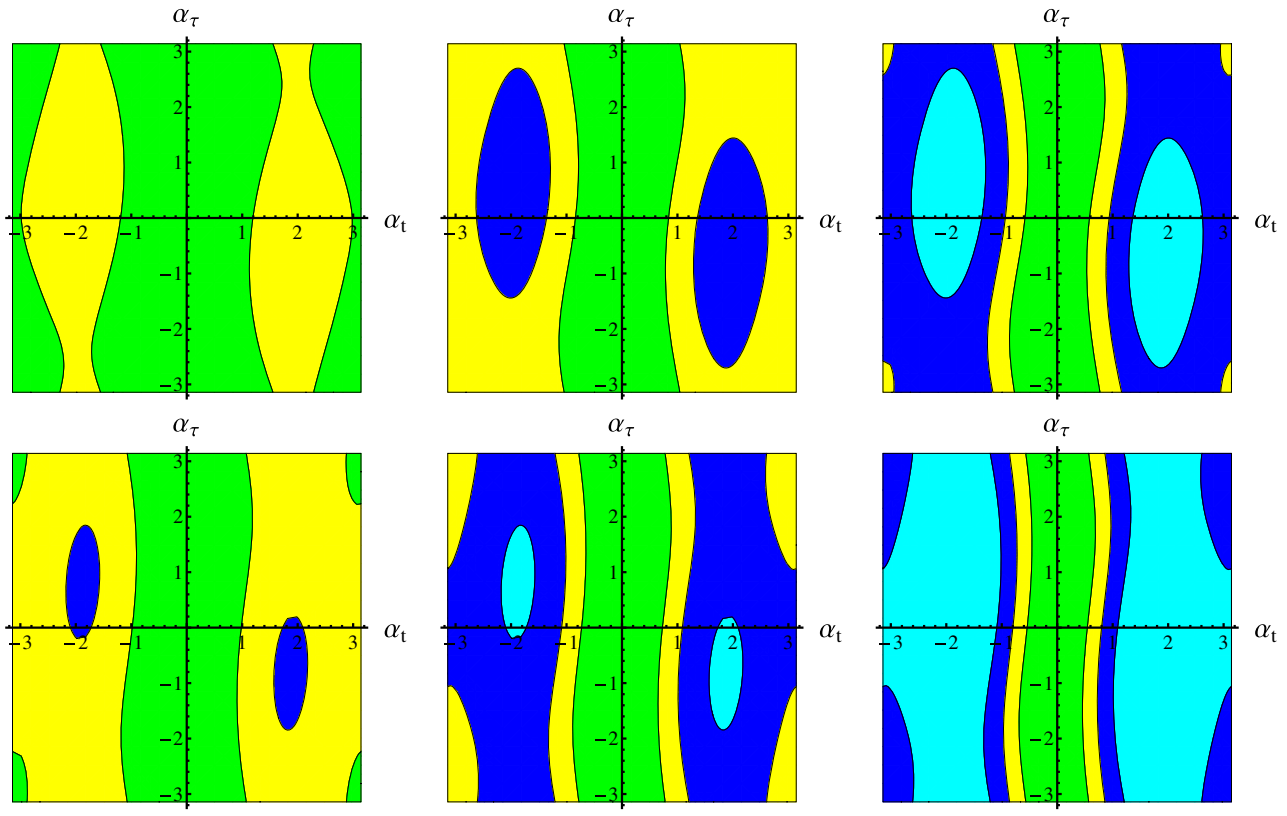

FIG. 8. $\mathrm{Br}(\tau \to \mu\gamma)$ distributions in the $\alpha_t - \alpha_\tau$ plane for $c_V = 0.5$ and $\Gamma_h/\Gamma_{h,\mathrm{SM}} = 0.3$, taking $|c_t| = 0.8$ in the first line and $|c_t| = 1.2$ in the second line, and $(\sigma_h/\sigma_{h,\mathrm{SM}})\mathrm{Br}(h \to \mu\tau) = (1.5, 3, 6) \times 10^{-3}$ from left to right. The green regions are for $\mathrm{Br}(\tau \to \mu\gamma) < 2 \times 10^{-10}$, the yellow regions are for $2 \times 10^{-10} \leq \mathrm{Br}(\tau \to \mu\gamma) < 5 \times 10^{-10}$, the blue regions are for $5 \times 10^{-10} \leq \mathrm{Br}(\tau \to \mu\gamma) < 10^{-9}$, and the cyan regions are for $10^{-9} \leq \mathrm{Br}(\tau \to \mu\gamma) < 2.4 \times 10^{-9}$.

For the $\tau \to \mu\gamma$ results, there are three typical cases listed in Table I in which a positive result means more than 3σ evidence and a negative result means an exclusion at 90% C.L., as usual. The typical choices are $\mathrm{Br}(\tau \to \mu\gamma) \sim 10^{-8}, 10^{-9}, 10^{-10}$ for each case. For the $h \to \mu\tau$ results, we should consider the cases for the LHC with positive and negative results separately.

A. LHC with positive result

A positive result in the $h \to \mu\tau$ search would mean direct evidence on LFV Higgs boson-μ-τ coupling. We take $(\sigma_h/\sigma_{h,\mathrm{SM}})\mathrm{Br}(h \to \mu\tau) = 1.5 \times 10^{-3}$, 3×10^{-3}, and 6×10^{-3} as benchmark points in this subsection.

First, consider scenario I in Sec. III, where the coupling strengths are close to those in the SM. Taking $c_V = \Gamma_h/\Gamma_{h,\mathrm{SM}} = 1$, $|c_t| = 1$, and 1.5, we show the $\mathrm{Br}(\tau \to \mu\gamma)$ distributions in the $\alpha_t - \alpha_\tau$ plane in Fig. 6, with the boundaries set according to the sensitivity of the SuperB factory. We can see that if $(\sigma_h/\sigma_{h,\mathrm{SM}})\mathrm{Br}(h \to \mu\tau) \gtrsim (2-3) \times 10^{-3}$, the typical predicted $\mathrm{Br}(\tau \to \mu\gamma)$ would reach the SuperB sensitivity, while if $(\sigma_h/\sigma_{h,\mathrm{SM}})\mathrm{Br}(h \to \mu\tau)$ was smaller, the $\tau \to \mu\gamma$ process would not be found at the SuperB factory.

Then we should focus on the green regions which show the cases with negative results at the SuperB factory. Here, we show the $\mathrm{Br}(\tau \to \mu\gamma)$ distributions in the $\alpha_t - \alpha_\tau$ plane in Fig. 7, with the boundaries set according to the sensitivity of the Super τ-charm factory. For $\mathrm{Br}(\tau \to \mu\gamma) \sim 10^{-9}$ or smaller, $|\alpha_t| \lesssim 1.5$ was favored. If the LHC is to give positive results, the typical predicted $\mathrm{Br}(\tau \to \mu\gamma)$ must reach the sensitivity of the Super τ-charm factory in this scenario. If the Super τ-charm factory were to give negative results, it would give strict constraints on the Higgs couplings.

In summary, for case I in Table I, if the SuperB factory were to give positive results in searching $\tau \to \mu\gamma$ (thus it must be discovered at the Super τ-charm factory as well), (α_t, α_τ) would fall into the blue or cyan regions in Fig. 6. The value of α_τ was usually free for a larger $|c_t|$ and $(\sigma_h/\sigma_{h,\mathrm{SM}})\mathrm{Br}(h \to \mu\tau)$, while $|\alpha_t| \gtrsim 1$ was favored for any case. While for case II in Table I the SuperB factory gave negative results but the Super τ-charm factory gave positive results, $|\alpha_t| \lesssim 1$ would be favored, and for most cases there would be no constraints on α_τ. For case III in Table I, where both factories gave negative results, larger $|\alpha_\tau|$'s and $|c_t|$'s would be favored.

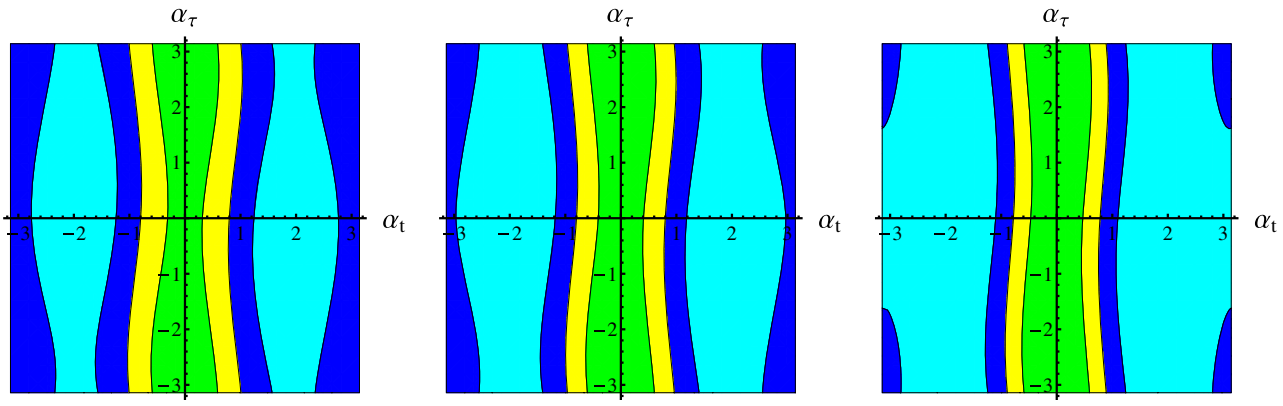

FIG. 9. $\mathrm{Br}(\tau \to \mu\gamma)$ distributions in the $\alpha_t - \alpha_\tau$ plane for $c_V = \Gamma_h/\Gamma_{h,\mathrm{SM}} = 1$, taking $|c_t| = 1$, 1.2, 1.5 from left to right. The green regions are for $\mathrm{Br}(\tau \to \mu\gamma) < 2 \times 10^{-10}$, the yellow regions are for $2 \times 10^{-10} \leq \mathrm{Br}(\tau \to \mu\gamma) < 5 \times 10^{-10}$, the blue regions are for $5 \times 10^{-10} \leq \mathrm{Br}(\tau \to \mu\gamma) < 10^{-9}$, and the cyan regions are for $10^{-9} \leq \mathrm{Br}(\tau \to \mu\gamma) < 2.4 \times 10^{-9}$.

Second, consider the Lee model, which is scenario II in Sec. III. In this scenario, both c_V and $\Gamma_h/\Gamma_{h,\mathrm{SM}}$ are smaller, where the predicted $\mathrm{Br}(\tau \to \mu\gamma)$'s are smaller. For example, taking $(\sigma_h/\sigma_{h,\mathrm{SM}})\mathrm{Br}(h \to \mu\tau) = 3 \times 10^{-3}$ as a benchmark point, the predicted $\mathrm{Br}(\tau \to \mu\gamma) \lesssim (0.8\text{–}1.6) \times 10^{-9}$, which cannot lead to a positive result at the SuperB factory.

We show the $\mathrm{Br}(\tau \to \mu\gamma)$ distributions in the $\alpha_t - \alpha_\tau$ plane in Fig. 8, with the boundaries set according to the sensitivity of the Super τ-charm factory, and all of the colored regions are for $\mathrm{Br}(\tau \to \mu\gamma) < 2.4 \times 10^{-9}$. Thus, case I in Table I would be disfavored.

In this scenario, the results for $\mathrm{Br}(\tau \to \mu\gamma)$ cannot reach the sensitivity of the SuperB factory, but they will reach the sensitivity of the Super τ-charm factory. If the Super τ-charm factory were to give negative results, as case III in Table I does, it would give strict constraints on the Higgs couplings so that $|\alpha_t| \lesssim 1$ would be favored, but the constraints on α_τ would be weak. However, if the Super τ-charm factory were to give positive results, as case II in Table I, larger $|c_t|$'s and α_t's would be favored.

B. LHC with negative result

In this subsection we choose $(\sigma_h/\sigma_{h,\mathrm{SM}})\mathrm{Br}(h \to \mu\tau) = 7.7 \times 10^{-4}$ as the LHC expected 95% C.L. upper limit together with the replacement (16). In scenario I in Sec. III, where the coupling strengths are close to those in the SM, the prediction is that $\mathrm{Br}(\tau \to \mu\gamma) \lesssim (1\text{–}2) \times 10^{-9}$, while in scenario II in Sec. III, as in the Lee model scenario, the prediction is that $\mathrm{Br}(\tau \to \mu\gamma) \lesssim (2\text{–}4) \times 10^{-10}$.

We should discuss the two scenarios separately. We show the $\mathrm{Br}(\tau \to \mu\gamma)$ distributions in the $\alpha_t - \alpha_\tau$ plane in Fig. 9 for scenario I and in Fig. 10 for scenario II, respectively. If the LHC gave negative results, case I in Table I cannot appear, thus we focus on cases II and III. For scenario I, if the Super τ-charm factory were to give negative results, $|\alpha_t| \lesssim (0.3\text{–}1)$ would be favored, or else the other regions would be favored. For scenario II, most regions are allowed for case III in Table I where both e^+e^- colliders gave negative results.

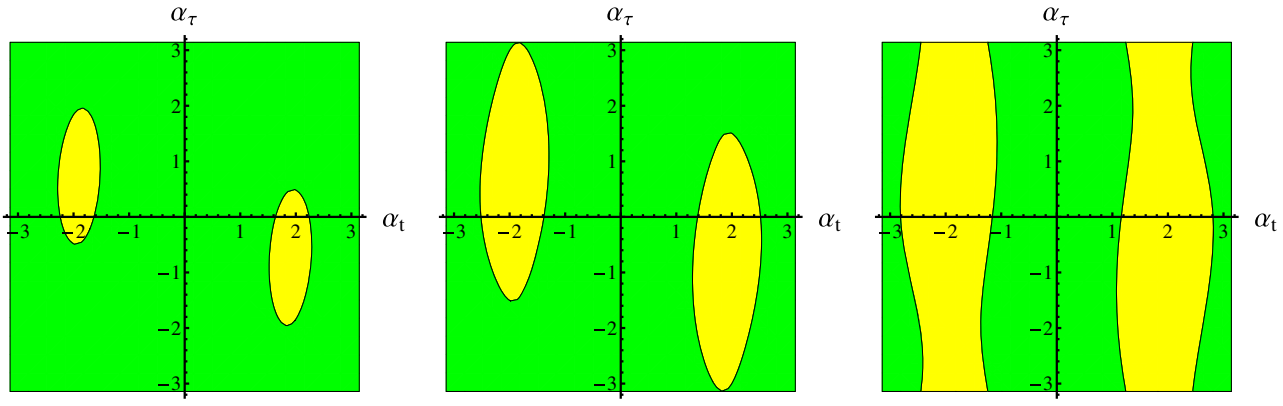

FIG. 10. $\mathrm{Br}(\tau \to \mu\gamma)$ distributions in the $\alpha_t - \alpha_\tau$ plane for $c_V = 0.5$ and $\Gamma_h/\Gamma_{h,\mathrm{SM}} = 0.3$, taking $|c_t| = 1$, 1.2, 1.5 from left to right. The green regions are for $\mathrm{Br}(\tau \to \mu\gamma) < 2 \times 10^{-10}$ and the yellow regions are for $2 \times 10^{-10} \leq \mathrm{Br}(\tau \to \mu\gamma) < 5 \times 10^{-10}$.

TABLE II. Short summary on all the future possibilities depending on the measurements $\mathrm{Br}(h \to \mu\tau)$ at the LHC and $\mathrm{Br}(\tau \to \mu\gamma)$ at the super B factory and super τ-charm factories and their corresponding implications.

	$\mathrm{Br}(h \to \mu\tau)$@LHC	$\mathrm{Br}(\tau \to \mu\gamma)$@SuperB	$\mathrm{Br}(\tau \to \mu\gamma)$ @Super τ-charm	Implications
P-I	positive	positive	positive	Scenario I favored; scenario II excluded.
P-II	positive	negative	positive	Both scenarios allowed; scenario I with small $\lvert\alpha_t\rvert$'s favored; scenario II with large $\lvert\alpha_t\rvert$'s favored.
P-III	positive	negative	negative	Scenario II favored; scenario I with small $\lvert\alpha_t\rvert$'s allowed.
P-IV	negative	positive	positive	Cannot be explained here.
P-V	negative	negative	positive	Scenario I with large $\lvert\alpha_t\rvert$'s favored; scenario II disfavored.
P-VI	negative	negative	negative	Scenario I with large $\lvert\alpha_t\rvert$'s disfavored; other parameter regions allowed.

V. CONCLUSIONS AND DISCUSSION

In this paper we discussed the Higgs boson-μ-τ coupling induced LFV decay processes $h \to \mu\tau$ and $\tau \to \mu\gamma$. For the latter process, the branching ratio is also closely related to the $ht\bar{t}$, $h\tau^+\tau^-$, and hW^+W^- couplings. We divided the BSM cases into two scenarios, namely, scenario I (II) with the Higgs coupling strengths close to (far away from) those in the SM, and for the latter scenario we took the Lee model as an example. We showed the possible numerical values of $\mathrm{Br}(\tau \to \mu\gamma)$ for different cases in Figs. 4–10.

If the future LHC run gives positive results on $h \to \mu\tau$, different measurements on $\mathrm{Br}(\tau \to \mu\gamma)$ at the SuperB factory and the Super τ-charm factory will distinguish the two scenarios or imply the favored parameter choices. For case I in Table I, with positive results from both the SuperB and Super τ-charm factories, scenario I would be favored, while scenario II would be disfavored or even excluded. For typical parameter choices, see the blue and cyan regions in Fig. 6 in details. For case II in Table I, with a negative result from the SuperB factory but a positive result from the Super τ-charm factory, both scenarios would be allowed and some constraints would be given on the Higgs couplings. See the blue and cyan regions in Figs. 7 and 8 for scenarios I and II, respectively, for detailed information on parameter choices. For scenario I, α_τ would be free in most cases, but regions near $(\alpha_t, \alpha_\tau) = (0, \pm\pi)$ would be disfavored for larger $|c_t|$'s and $\mathrm{Br}(h \to \mu\tau)$'s. For scenario II, $|\alpha_t| \gtrsim 1$ would be favored and thus implies large CP violation in $ht\bar{t}$ coupling. For case III in Table I, with negative results from both the SuperB and Super τ-charm factories, scenario II would be favored, but scenario I would not be excluded. See the green regions in Figs. 7 and 8 for scenarios I and II, respectively.

If the future LHC run gives negative results on $h \to \mu\tau$, case I in Table I will not be explainable. If case I were really to happen, we would need other models. For case II in Table I, scenario I with $|\alpha_t| \gtrsim (0.5\text{–}1)$ would be favored, which implies large CP violation in the $ht\bar{t}$ coupling, while there would be almost no constraints on α_τ. See Fig. 9 for details. For case III in Table I, nothing about LFV is to be seen at future colliders. Scenario I with $|c_t| \gtrsim (0.5\text{–}1)$ would be excluded, while other regions for both scenarios would be allowed.

In Table II we summarize the implications corresponding to all six future possibilities, depending on the measurements of $\mathrm{Br}(h \to \mu\tau)$ at the LHC and $\mathrm{Br}(\tau \to \mu\gamma)$ at the SuperB and Super τ-charm factories. With the help of future measurements on LFV processes $h \to \mu\tau$ and $\tau \to \mu\gamma$ at both high and low energy colliders, in most cases we would be able to distinguish different BSM scenarios or set constraints on the Higgs couplings. P-IV in Table II would be strange. If this is really the case in the future, the Higgs induced LFV would not be the underlying reason. It would require another mechanism beyond the Higgs sector to generate large enough LFV processes, such as $\tau \to \mu\gamma$.

ACKNOWLEDGMENTS

We thank Gang Li, Yuji Omura, and Chen Zhang for the helpful discussions. This work was supported in part by the Natural Science Foundation of China (Grants No. 11135003 and No. 11375014).

[1] N. Cabbibo, Phys. Rev. Lett. **10**, 531 (1963); M. Kobayashi and T. Maskawa, Prog. Theor. Phys. **49**, 652 (1973).
[2] S. L. Glashow, J. Iliopoulos, and L. Maiani, Phys. Rev. D **2**, 1285 (1970).
[3] W. J. Marciano and A. I. Sanda, Phys. Lett. **67B**, 303 (1977).
[4] B. Pontecorvo, Zh. Eksp. Teor. Fiz. **33**, 549 (1957). [Sov. Phys. JETP **6**, 429 (1957)]; Z. Maki, M. Nakagawa, and S. Sakata, Prog. Theor. Phys. **28**, 870 (1962).
[5] K. A. Olive *et al.* (Particle Data Group), Chin. Phys. C **38**, 090001 (2014).
[6] K. Hayasaka *et al.* (Belle Collaboration), Phys. Lett. B **666**, 16 (2008); B. Aubert *et al.* (*BABAR* Collaboration), Phys. Rev. Lett. **104**, 021802 (2010).
[7] J. Adam *et al.* (MEG Collaboration), Phys. Rev. Lett. **110**, 201801 (2013).
[8] J. Brodzicka *et al.* (Belle Collaboration), Prog. Theor. Exp. Phys. **2012**, 04D001 (2012).
[9] T. Aushev *et al.*, KEK Report No. 2009-12, 2010.
[10] SuperB Collaboration, Reports No. INFN/AE-10/2, No. LAL-110, and No. SLAC-R-952, 2010.
[11] A. M. Baldini *et al.* (MEG Collaboration), arXiv: 1301.7225.
[12] S.-H. Zhu, arXiv:1410.2042.
[13] ATLAS Collaboration, Phys. Lett. B **716**, 1 (2012).
[14] CMS Collaboration, Phys. Lett. B **716**, 30 (2012).
[15] M. Flechl (for the ATLAS and CMS Collaborations), J. Phys. Conf. Ser. **631**, 012028 (2015).
[16] CMS Collaboration, Phys. Lett. B **749**, 337 (2015).
[17] ATLAS Collaboration, J. High Energy Phys. 11 (2015) 211.
[18] G. C. Branco, P. M. Ferreira, L. Lavoura, M. N. Rebelo, M. Sher, and J. P. Silva, Phys. Rep. **516**, 1 (2012).
[19] J. D. Bjorken and S. Weinberg, Phys. Rev. Lett. **38**, 622 (1977).
[20] D. Aristizabal Sierra and A. Vicente, Phys. Rev. D **90**, 115004 (2014).
[21] D. Das and A. Kundu, Phys. Rev. D **92**, 015009 (2015).
[22] F. J. Botella, G. C. Branco, M. Nebot, and M. N. Rebelo, Report No. IFIC-15-62, 2015.
[23] J. Heeck, M. Holthausen, W. Rodejohann, and Y. Shimizu, Nucl. Phys. **B896**, 281 (2015).
[24] A. Crivellin, G. D'Ambrosio, and J. Heeck, Phys. Rev. Lett. **114**, 151801 (2015).
[25] A. Crivellin, G. D'Ambrosio, and J. Heeck, Phys. Rev. D **91**, 075006 (2015).
[26] Y.-N. Mao and S.-H. Zhu, Phys. Rev. D **90**, 115024 (2014).
[27] T. D. Lee, Phys. Rev. D **8**, 1226 (1973).
[28] L. de Lima, C. S. Machado, R. D. Matheus, and L. A. F. do Prado, J. High Energy Phys. 11 (2015) 074.
[29] I. Doršner, S. Fajfer, A. Greljo, J. F. Kamenik, N. Košnik, and I. Nišandžic, J. High Energy Phys. 06 (2015) 108.
[30] K. Cheung, W.-Y. Keung, and P.-Y. Tseng, Phys. Rev. D **93**, 015010 (2016).
[31] B. Bhattacherjee, S. Chakraborty, and S. Mukherjee, arXiv:1505.02688.
[32] Y. Omura, E. Senaha, and K. Tobe, J. High Energy Phys. 05 (2015) 028.
[33] G. Blankenburg, J. Ellis, and G. Isidori, Phys. Lett. B **712**, 386 (2012).
[34] R. Harnik, J. Kopp, and J. Zupan, J. High Energy Phys. 03 (2013) 026.
[35] C.-J. Lee and J. Tandean, J. High Energy Phys. 04 (2015) 174.
[36] T. P. Cheng and M. Sher, Phys. Rev. D **35**, 3484 (1987).
[37] E. Levichev, Phys. Part. Nucl. Lett. **5**, 554 (2008).
[38] A. V. Bobrov and A. E. Bondar, Nucl. Phys. B, Proc. Suppl. **253–255**, 199 (2014).
[39] J. P. Ma and C. H. Chang, Sci. China Phys., Mech. Astron. **53**, 1947 (2010).
[40] LHC Higgs Cross Section Working Group, Report No. CERN-2013-004, 2013.
[41] S. M. Barr and A. Zee, Phys. Rev. Lett. **65**, 21 (1990); **65**, 2920 (1990).
[42] S. Davidson and G. Grenier, Phys. Rev. D **81**, 095016 (2010).
[43] D. Chang, W.-S. Hou, and W.-Y. Keung, Phys. Rev. D **48**, 217 (1993).
[44] J. Kopp and M. Nardecchia, J. High Energy Phys. 10 (2014) 156.